CHAPTER 17

Micropatterning Approaches for Cardiac Biology

Nicholas A. Geisse, Adam W. Feinberg, Po-ling Kuo, Sean P. Sheehy, Mark-Anthony Bray, and Kevin Kit Parker

17.1 Introduction

Our understanding of the relationship between cell boundary conditions and cell function has been greatly accelerated with the implementation of soft lithography in order to control the cellular microenvironment. Using these techniques, it has been shown that imposed boundary conditions can influence biological processes as diverse as gene-expression profiles and cell fates [1], subcellular localization of chemical signaling pathways and organization of cytoskeletal architecture [2], and the direction and magnitude of cell-tractional forces [3]. Beyond insights at the single-cell level, soft lithography has been applied to the study of cell-cell interactions and to the generation of engineered tissue constructs [4, 5]. Indeed, engineering the cell microenvironment provides investigators unprecedented abilities to investigate the relationship between cell structure and function. These structure-function relationships are no less important in the myocardium, where the relationship between cell shape and boundary conditions is crucial for the proper functioning of both the individual cardiac myocyte and the tissue syncytium. For example, mammalian ventricular cardiac myocytes in vivo are generally cylindrical, with approximate dimensions of 100 to 120 μm in length, 15 to 20 μm in width, and 10 μm in thickness. Cardiac myogenesis occurs by developing electrical and mechanical connections between adjacent myocytes while maintaining uniaxial alignment with respect to one another. This uniformity of structure is supported by experimental data and computer-modeling studies, which hypothesize that the shape and connectivity of individual myocytes greatly influences electrical-impulse propagation throughout the myocardium [6–8]. Although cellular dimensions vary across species and individuals, healthy myocytes generally have a length:width (or aspect) ratio of ~7:1. Various cardiomyopathies are accompanied by deviations from this ratio [9], and myocyte shape changes are concomitant with declining contractile performance. These maladaptive responses may occur due to a variety of stimuli [10], but at present the causal relationship between this structural change and dysfunction at the myocyte, tissue, and organ level has yet to be directly established.

Microscale surface-engineering techniques have laid the foundation for investigating the role that cellular boundary conditions play in potentiating various aspects of myocyte physiology and pathophysiology and have had a long evolution

due to the difficulty of creating micro- and nanoscale features for cell attachment. Early studies focused on creating mechanically microtextured cell-culture substrates for patterned cell growth. One of the earliest techniques, developed by Lieberman et al., focused on creating long, cylindrical fibers of a cardiac myocyte preparation in order to perform electrical measurements, and these were created by culturing myocytes on manually cut trenches in soft agar culture substrates [11, 12]. Using this technique, Lieberman et al. were able to create strands of electrically conductive cardiac tissue that could be investigated with electrophysiology techniques. Other methods of manual alteration of the cell microenvironement include microabrasion (a method reproduced in Section 17.3.1 of this chapter), where pliant culture substrates such as polystyrene or polyvinylchloride are mechanically scratched, providing three-dimensional surface topography for directing cell growth and spatially orienting cell-cell communication [13].

Despite these methods for altering the cell-culture microenvironment to spatially direct and organize cardiac myocyte growth, it was not until the development of photolithography and soft lithography techniques [14] and their subsequent applications to biological samples [15] that the investigator was given the ability to design surfaces with micron to nanometer precision. Here, surfaces composed of a polymer photoresist are etched by exposure to ultraviolet light shone through a photomask. The design placed on the photomask is transferred to the substrate by either stabilizing or destabilizing the photoresist, depending on the type used. After processing, the surface provides a near perfect relief or reverse-relief of the photomask, which can be designed with micron-sized features with little loss of pattern fidelity. Adaptation of this technique utilized the precise spatial control afforded by photolithography, and implementation technology for controlling the cardiac myocyte microenvironment was pioneered by Kleber et al. [16–18], who created patterned surfaces in biocompatible photoresist in order to study the relationship between electrical conduction and tissue structure. With these techniques, it is possible to control the size of an engineered myocyte strand to the resolution of a cell width, while recapitulating the anisotropic cellular architecture found in the in vivo myocardium. This is important since it is thought that the structure and cytoskeletal architecture of the cardiac myocyte greatly influence, if not determine, myocyte contractility and intercellular electrical coupling [19–21]. A wide variety of stimuli can evoke physiological responses in the heart, and, in particular, it has been shown that mechanical forces play a central role in cardiac myocyte regulation and function [10]. However, the relationship between cardiac myocyte shape, cytoskeletal architecture, and physiology remains unclear due to the difficulty of culturing cardiac myocytes and controlling the cellular microenvironment in vitro.

In the following discussion, we describe several techniques adapted for use in our laboratory to study structure-function relationships in single cardiac myocytes and two-dimensional cardiac tissue constructs. We include a discussion of myocyte isolation and culture maintenance and the special considerations needed for cardiac myocytes. Central to our structure-function studies is the use of the microcontact printing (μCP) technique in order to control myocyte shape by controlling the availability and spatial distribution of extracellular matrix (ECM). The μCP technique allows for fabrication of shape-controlled myocytes and two-dimensional tissues, and it is shown that the boundary conditions determined by μCP influence

intercellular organization. Coupling the μCP technique with fluorescence microscopy on deformable substrates and with novel image-processing techniques, the tractional forces exerted by the myocyte onto its substrate can be observed. We close this discussion with a look at the prospective techniques in cell and tissue engineering.

17.2 Isolation and Culture of Cardiac Myocytes

In vitro cell-culture models are a powerful tool for studying the activities and characteristics of cellular processes and how they respond to various controlled conditions. Isolated adult rat cardiac myocytes have mature myofibrillar networks that maintain their structure and function when enzymatically dissociated from the whole heart. As such, adult cardiac myocytes settle on to surfaces but do not respond to chemical or mechanical microenviromental cues either by forming focal contact adhesions with the substrate or by conforming to the shape of the substrate. This inability to form attachments with the substrate limits adult myocyte viability to approximately one day in vitro, after which myocyte viability decreases while the rate of dedifferentiation increases. In contrast, freshly isolated neonatal rat ventricular myocytes (NNRVMs) have a more malleable cytoskeletal structure, allowing them to conform to the chemical and mechanical characteristics of the cell-culture substrate. This flexibility, coupled with techniques to engineer the cell microenvironment, has resulted in the use of NNRVMs for the study of various myocardial structural and functional properties, such as action potential duration [22], impulse propagation [17], calcium-induced calcium release [23], signaling pathways, and gene expression [24]. Additionally, cultured NNRVMs have been used to develop models for the study of pathological conditions in the heart, like ischemia-reperfusion injury [25], hypertrophy [26], and arrythmogenesis [13].

Cultured NNRVMs are an excellent cell type for in vitro cardiac research because they retain a limited measure of developmental plasticity that their adult counterparts do not and because they can survive in culture for longer periods. Good sterile technique and swift completion of the culture process are important to ensure maximum yield and longevity of healthy, viable myocytes. The procedure that follows is briefly outlined in Figure 17.1. All procedures should be conducted within a biosafety cabinet using supplies and equipment that have been autoclave-sterilized to prevent contamination. Cardiac myocytes are postmitotic cells and have a limited lifetime in vitro dependent upon the conditions under which they are maintained, and this is further complicated by the temporal duration of attachment compared to other adherent cells, such as fibroblasts (days compared to hours, respectively). All procedures described in this text are in compliance with the Harvard University Care and Use Committee, and experiments presented here were performed within the appropriate approved guidelines.

17.2.1 Harvesting and Isolating NNRVMs

Prior to the myocyte isolation and culture procedure, the appropriate culture medium must be prepared in order to preserve the cells during isolation. An excel-

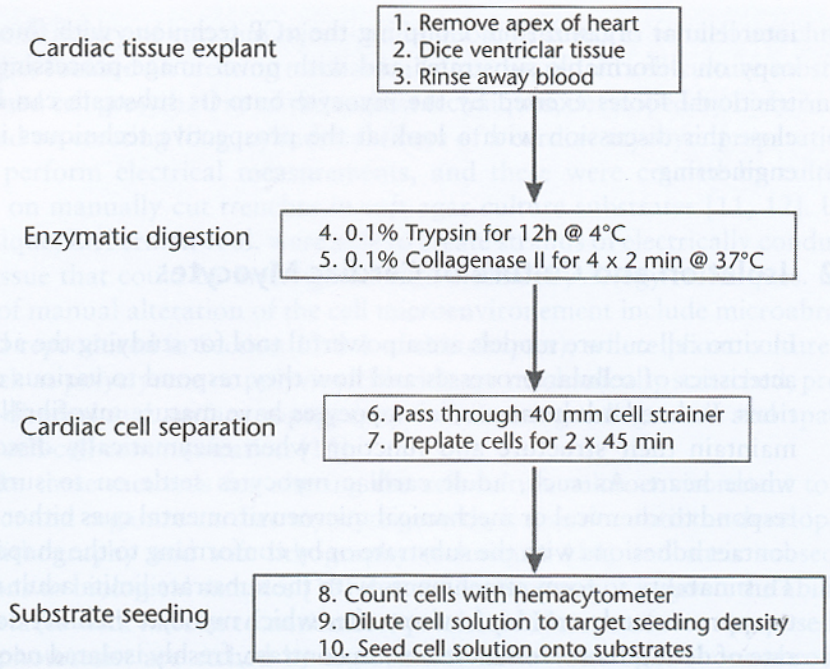

Figure 17.1 *Flowchart for isolation of NNRVMs.* Full isolation and culture of NNRVMs involves several steps performed over the course of approximately eighteen hours. The procedure involves manual tissue dissection, followed by enzymatic degradation to separate cells from the ECM and each other. Further steps are taken to remove nonmyocyte adherent cells. See text for details.

lent preservative solution is made by supplementing medium 199 with 10 mM HEPES buffer solution, 10mM MEM nonessential amino acids, 2 mM L-glutamine solution, 20 mM glucose, 1.5 μM vitamin B12, 50 units/mL penicillin, and 10 percent fetal bovine serum. Isolation of cells begins with extraction from the organism, which must be sterilized with ethanol to minimize the transfer of contaminants from the surface of its skin onto the surgical equipment. In general, the organism is sacrificed via decapitation, and the heart is removed with a mid-sternal ventral incision. Once the heart is extracted, ventricular tissue is excised and rinsed in Hank's Balanced Salt Solution (HBSS). Homogenization of the tissue is done manually with scissors or scalpels, and the tissue is then diced and kept submerged in HBSS. Subsequently, the tissue is digested in a solution of 0.1 percent trypsin in HBSS and incubated with agitation for approximately twelve hours at 4°C. After digestion, the tissue is serially dissociated into individual cells by multistep incubation in a 0.1 percent collagenase type II solution for two minutes each at 37°C.

Cells are isolated and resuspended by centrifugation and strained in order to remove large, undigested sections of tissue. Perhaps the greatest difficulty faced when making NNRVM preparations is the presence of contaminating cells, such as fibroblasts, vascular smooth muscle, and capillary epithelial cells. In order to minimize these contaminations, the cell solution can be preplated twice for forty-five minutes each time in 75 mm^2 tissue-culture flasks. Once the preplating steps are complete, the myocyte solution is ready to be diluted and plated onto a variety of microengineered cell-culture substrates.

17.3 Engineering the Cellular Microenvironment In Vitro

17.3.1 Microabrasion of the Cardiac Myocyte Culture Substrate

A simple method for controlling tissue anisotropy is via mechanical etching of the culture substrate, which provides physical cues for myocyte attachment and assembly [13]. Unlike methods that utilize large trenches either cut into a substrate [11, 12] or fabricated via photolithography [16–18], microabrasions that can guide myocyte orientation can be etched into the surface using commonly available materials. Polyvinyl chloride (PVC) transparent coverslips are abraded using fine, one hundred grit sandpaper. Atomic force microscopy shows that a one-pass abrasion creates individual trenches distributed across the surface that have a depth and peak of ~0.5 μm from the surface [Figure 17.2(a)]. Multipass abrasions generate trenches along the entire surface that are ~3.0 to 4.0 μm in height [Figure 17.2(b)]. Both substrates can be treated with a solution of fibronectin (FN) and used for cell plating. Cardiac myocytes that are seeded onto these substrates show an alignment with the

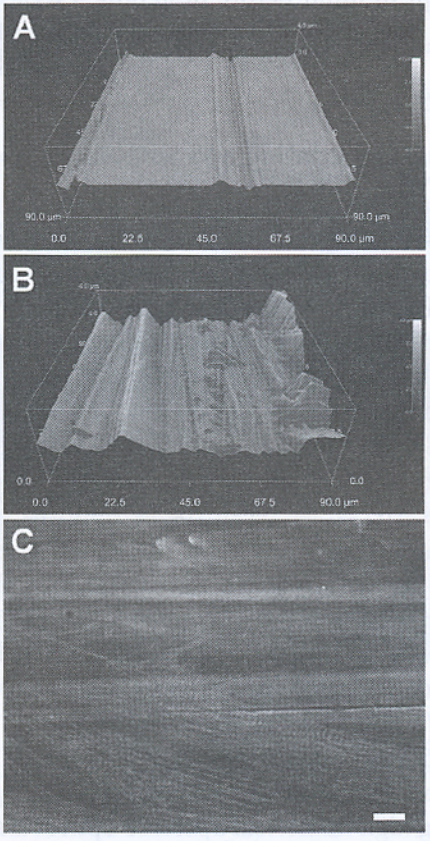

Figure 17.2 *Microabrasion of the cardiac myocyte culture substrate.* Atomic force micrographs of microabraded PVC coverslips show geometrical cues in the direction of the abrasion. (a) Single-pass microabrasion creates small, individual trenches across the surface that are approximately 0.5 μm deep. (b) Multiple-pass microabrasion results in a completely rough culture substrate with trenches in the direction of the abrasion. Height variation across this substrate is 3.0 to 4.0 μm. c) Cardiac myocytes cultured on these substrates and stained for actin filaments, sarcomeric α-actinin, and the nucleus show myofibrillar alignment along the direction of the microabrasions, visualized as the dark horizontal line. Scale bar = 10 μm.

microabraded lines, as shown in Figure 17.2(c). Microabraded trenches are easily identified in both the transmitted light (not shown) and the fluorescence images, as shown by the dark horizontal line in Figure 17.2(c). Myofibrillar staining of actin (green) and sarcomeric α-actinin (red) show that these structures align in parallel with and perpendicularly to the microabraded lines, respectively. A similar technique has been successfully used to generate constructs for the measurement of action potential propagation in two-dimensional ansisotropic tissues [13]. Although this technique is suitable for creating anisotropic tissues, microabrasion does not allow the investigator control over cell geometry and tissue anisotropy on the scale of single-cell widths.

Our experience has led us to the conclusion that μCP is generally superior both to the microabrasion technique and to other soft lithography techniques, such as microfluidics, for building ECM templates of myocyte shape and two-dimensional tissue architecture. In μCP, a stamp is used to "ink" a surface with a pattern of ECM proteins that the dissociated myocytes settle on and remodel in response to the geometric cues in the ECM and their neighboring cells. A description of the principles that must be kept in mind before designing a μCP pattern, as well as a discussion of the chemical properties of the elastomer, is useful prior to explanation of this technique.

17.3.2 Microcontact Printing and Soft Lithography

One of the primary advantages of microcontact printing is that it allows for cardiac myocytes to be grown on layers of a silicone polymer. In many cases, polydimethylsiloxane (PDMS) is the silicone of choice. The mechanical properties of PDMS ($E \sim 1$ MPa) allow for cardiac myocytes to be cultured in vitro for longer periods than on glass ($E \sim 70$ GPa) or tissue-culture-grade polystyrene ($E \sim 3$ GPa). Myocytes rebuild their myofibrillar networks upon being seeded onto surfaces, forming focal contact adhesions and adopting a cell shape dependent on the two-dimensional boundary conditions of the ECM. Myocyte contractions result in cyclic loading of the focal contact adhesions between the myocytes and the surface, generating large stresses between the cell and ECM, between the ECM and substrate, and within the substrate. The delamination is believed to be caused by enzymatic degradation of the ECM by matrix metalloproteinases produced by the myocytes and/or fibroblasts and likely accelerated by the high stress conditions. In contrast, the lower modulus PDMS surface absorbs some of the strain, delaying myocyte delamination until approximately nine days in vitro, thereby extending the experimental window.

One of the critical advantages of μCP is that it allows for patterned cells to be grown on traditional culture substrates, facilitating analysis by a variety of techniques, including high numerical aperture optical and fluorescence microscopy. Previous techniques utilized alkane-thiol-based μCP printing strategies to control cell shape [2]. These techniques are less than ideal for many live-cell-imaging methods due to the opacity of the culture substrate. By exploiting the control of the wettability of PDMS [27], μCP can be performed using either glass or PDMS as a cell-culture substrate, both of which are transparent and permit live-cell fluores-

cence imaging. For our studies, we perform μCP on glass microscope coverslips that are coated with a thin (~17 μm) layer of PDMS.

Standard soft lithography procedures are used to fabricate the PDMS stamps used for microcontact printing [14]. A graphical overview of the process from stamp production to cell seeding is presented in Figure 17.3(a). Silicon wafers (3″ diameter) are spin-coated with a 2 to 3 μm thick layer of SU-8 photoresist (MicroChem Corp., Newton, MA), followed by a prebake at 65°C for two minutes

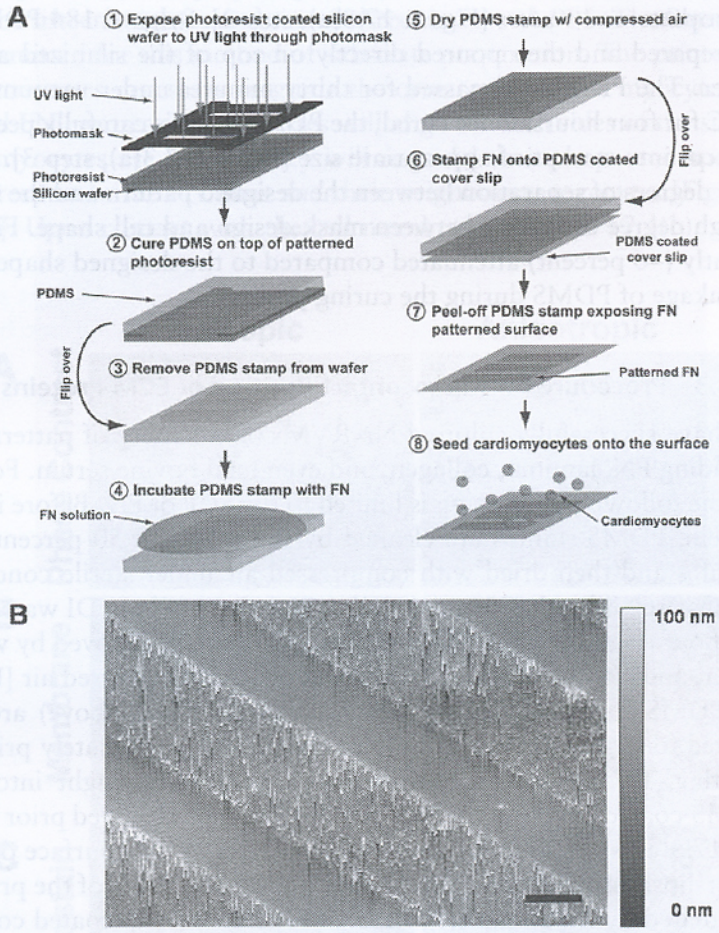

Figure 17.3 *Schematic of the stamp fabrication and microcontact printing process for ECM proteins on to PDMS coated coverslips*: (a) Overview of the process: (1) A silicon wafer is coated in photoresist and photolithographically patterned by exposing the photoresist with ultraviolet light passed through a photomask. (2) The photoresist is developed, thus removing the ultraviolet-exposed regions, and the remaining topography is copied by casting PDMS prepolymer on top. (3) The cured PDMS is peeled off of the silicon wafer, creating a stamp with microtopography. (4) The PDMS stamp is inked by incubation with an ECM protein solution for one hour. (5) The ECM protein solution is rinsed off in ddH_2O and then dried under compressed air. (6) The inked PDMS stamp is placed pattern-side down on the PDMS-coated coverslip, transferring the ECM protein to the substrate in defined patterns in a process adapted from [27]. (8) Once the ECM patterned coverslip is washed in buffer, myocytes are seeded. (b) Atomic force deflection micrograph of 20 μm–wide micropatterned lines of FN reveal a thin, ~3 nm layer of protein on the PDMS surface.

and soft-bake at 95°C for four minutes. Photoresist-coated silicon wafers are transferred to a mask aligner, where they are patterned via exposure to ultraviolet light through a photomask (Karl Suss MicroTec, Munich, Germany) using contact photolithography [Figure 17.3(a), step 1]. After exposure, wafers are developed in propylene glycol monomethyl ether acetate, then washed for one minute in isopropyl alcohol, resulting in a micropatterned layer of SU-8 photoresist on top of the silicon wafer. The surface of the wafer is then passivated by silanazation to prevent the PDMS from permanently binding to the wafer during stamp preparation. PDMS stamps for microcontact printing are prepared by curing PDMS on top of the micropatterned wafers [Figure 17.3(a), step 2]. Sylgard 184 PDMS (Dow Corning) is prepared and then poured directly on top of the silanized and micropatterned wafer. The PDMS is degassed for thirty minutes under vacuum and then cured at 65°C for four hours. Once cured, the PDMS layer is carefully peeled off of the wafer and cut into stamps of appropriate size [Figure 17.3(a), step 3]. Although there are four degrees of separation between the designed pattern and the final stamp, there is a high degree of fidelity between mask design and cell shape. Final cell size is only slightly (~6 percent) attenuated compared to the designed shape, mostly due to the shrinkage of PDMS during the curing process.

17.3.3 Procedure for Microcontact Printing of ECM Proteins

We have successfully cultured NNRVMs on a variety of patterned ECM proteins, including FN, laminin, collagen, and even fetal bovine serum. For purposes of clarity, the following discussion is limited to the μCP of FN. Before incubation with the protein, PDMS stamps are cleaned by sonication in 50 percent ethanol for thirty minutes and then dried with compressed air under sterile conditions. The PDMS stamps are "inked" with a droplet of 50 μg/ml of FN in DI water and incubated for one hour [Figure 17.3(a), step 4]. Excess protein is removed by washing twice in DI water, and stamps are then dried using filtered compressed air [Figure 17.3(a), step 5]. PDMS-coated coverslips (prepared as described above) are ultraviolet-ozone treated for eight minutes to sterilize the surface immediately prior to microcontact printing. Under sterile conditions, the stamp is brought into contact with the PDMS-coated coverslip for two minutes and then removed prior to cell seeding [Figure 17.3(a), steps 6–8]. Proteins are transferred to the surface of the PDMS coated coverslips, forming an approximately 3 nm–thick layer of the protein in the pattern designated by the stamp [Figure 17.3(b)]. The PDMS-coated coverslip is now patterned with protein and is further functionalized as per the specific experimental protocol. To restrict cell growth to the protein-patterned area, the PDMS-coated coverslip is incubated in a blocking solution of 1 percent (w/v) Pluronics F-127 (BASF Corp., Mount Olive, NJ) in DI water solution for fifteen minutes and then washed three times with phosphate buffered saline (PBS). The stamped, PDMS-coated coverslips can be stored covered in PBS for up to forty-eight hours prior to seeding with cardiac myocytes. The seeding density for myocytes on individual islands with liberal spacing in between the islands on a 25 mm coverslip may be on the order of 10^5 myocytes, whereas for a two-dimensional anisotropic tissue, 10^6 myocytes may be required. Once prepared, myocytes can be plated at an appropriate density determined by experimental needs.

Prior to μCP, studies requiring contiguous cardiac tissue assembled from NNRVMs were generally isotropic [Figure 17.4(a–c), left panels] cultured on an isotropic pattern of ECM. Now, with a μCP template, a two-dimensional anisotropic tissue that more accurately depicts the laminar structure of the ventricles is possible [Figure 17.4(a–c), right panels]. Fabrication of anisotropic two-dimensional tissues is possible by following μCP of FN lines with a step designed to provide a background layer of FN. This background layer allows myocytes to adhere between the patterned lines. After the PDMS-coated coverslip is stamped, the coverslip is coated with a layer of low-density FN (2.5 μg/ml of FN in DI water) for fifteen minutes and rinsed three times with PBS. The Pluronics blocking step is omitted for this method of substrate preparation. The printed lines provide geometric cues necessary to guide the orientation of the myocytes, while the background FN ensures that myocytes will align on both sides of the stamped line. When the myocytes are seeded, they will remodel their shape and spontaneously align with respect to the FN lines and their neighboring myocytes [Figure 17.4(a), right panel]. Upon contact with the cell membranes [Figure 17.4(b), right panel],

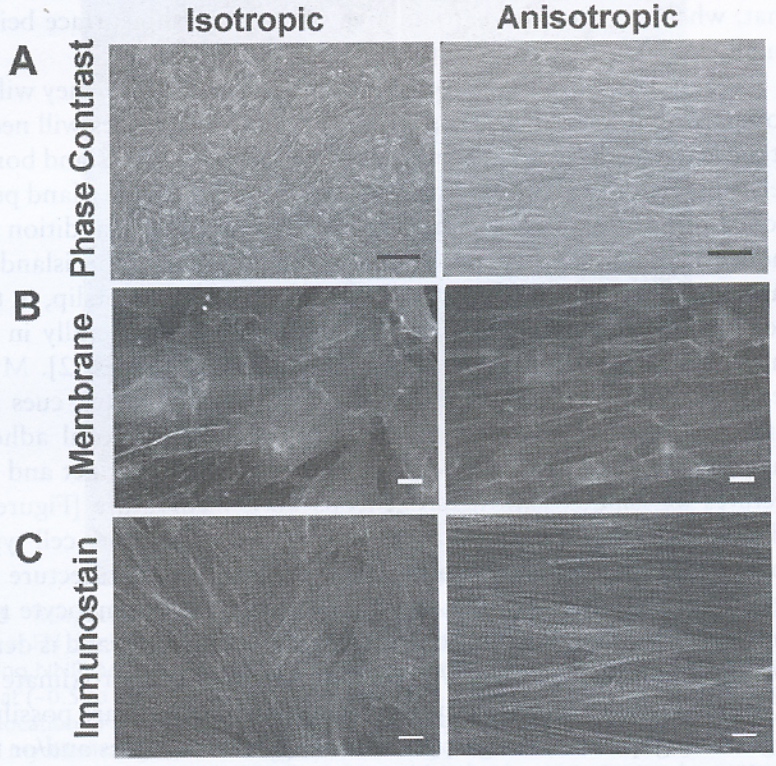

Figure 17.4 *Myofibrillar architecture of two-dimensional tissue constructs*: (a, left) NNRVMs cultured according to the above protocol on uniform layers of FN exhibit isotropic cellular orientation when compared to (a, right) NNRVMs cultured on lines of FN that result in an anisotropic orientation, as shown by phase-contrast microscopy. (b) Staining the myocytes with a fluorescent membrane dye (di-8-ANNEPS, Molecular Probes) shows that the myocyte edges also respond to geometrical cues in the FN. (c) Fixed and stained isotropic (left) and anisotropic (right) reveal that myofibrillar architecture is also oriented based on these cues. Immunostain labels for actin filaments, sarcomeric α-actinin, and the nucleus were used to visualize myofibrils and the nuclei. Scale bars for (a) are 100 μm; scale bars for (b) and (c) are 10 μm.

myocytes will form gap-junction connections with neighboring myocytes. As this electrical continuity is achieved, myocytes begin to beat spontaneously, inducing sarcomeregenesis and the reorganizing of existing sarcomeres. When this process is complete, the sarcomere Z-lines, as indicated by sarcomeric α-actinin immunostaining, will be observed to register both intra- and intercellularly with an orientation perpendicular to the longitudinal axis of the myocytes and the tissue that they form [Figure 17.4(c), right panel]. On the rigid PDMS coverslip, their contraction will be isometric but can be detected by the displacement of the myocyte nucleus.

Previous cardiac biology on cultured myocytes relied on either freshly harvested myocytes or pleomorphic myocytes [Figure 17.5(a)]. With the implementation of μCP for engineering the cardiac myocyte microenvironment, a variety of myocyte shapes are now possible [Figure 17.5(b–f)]. When patterning single myocytes, it is important that the mask design take into account the requirement of large numbers of cardiac myocytes to establish the paracrine signaling networks required for myocyte survival in vitro. This can be accomplished either by seeding a high density of myocyte islands per unit area or by the inclusion of a "conditioning layer" in the design, as noted by Rohr, Scholly, and Kleber [16]. This layer is a region of the mask that, when stamped, leads to an area of the coverslip surface being occupied by a small, confluent region of isotropic myocytes.

When the myocytes make contact with the FN islands, they will spread slowly in comparison to other cell types. This is because sarcomeres will need to disassemble at the leading edge where the myocyte is reaching for the island border. Unlike other cell types, myocytes will not extend lamellipodia from the island periphery. As mentioned previously, myocytes may require coaxing by the addition of epinephrine to induce beating and hypertrophy in order to achieve the island shape. Whereas myocyte shape is well controlled in the plane of the coverslip, in the vertical direction the nucleus will appear as a prominent bump, generally in the center of the myocyte [Figure 17.5(b)], as observed in other cell types [2]. Myocytes will then reorganize their cytoskeleton with respect to the geometric cues in the FN island. After the actin network is stabilized and secured by focal adhesion complexes, myofibrillogenesis will follow the actin template for distinct and repeatable architectures on islands with heterogeneous border curvature [Figure 17.5(c, d)]. On islands with homogeneous curvature, myocytes, like other cell types, will lack the spatial cues required to stabilize their cytoskeletal architecture [Figure 17.5(e)], resulting in a widely varying myofibrillar pattern from myocyte to myocyte. As in the two-dimensional tissue, contraction will be isometric and is detectable by monitoring nuclear displacement. Arrays of myocytes that approximate the broad ranges of aspect ratios observed in the ventricular myocardium are possible and will allow high-throughput screening of pharmacological candidates and/or toxins, as well as facilitate statistical studies of myocyte behavior [Figure 17.5(f)]. In this regard, the isometric contraction of the myocytes on the rigid substrate is advantageous during high-speed fluorescent video microscopy with Ca^{2+} indicators or voltage-sensitive dyes due to lack of motion artifact. For contractility studies, we have adapted the traction force microscopy technique [28] for the unique requirements of the rapidly contracting myocyte.

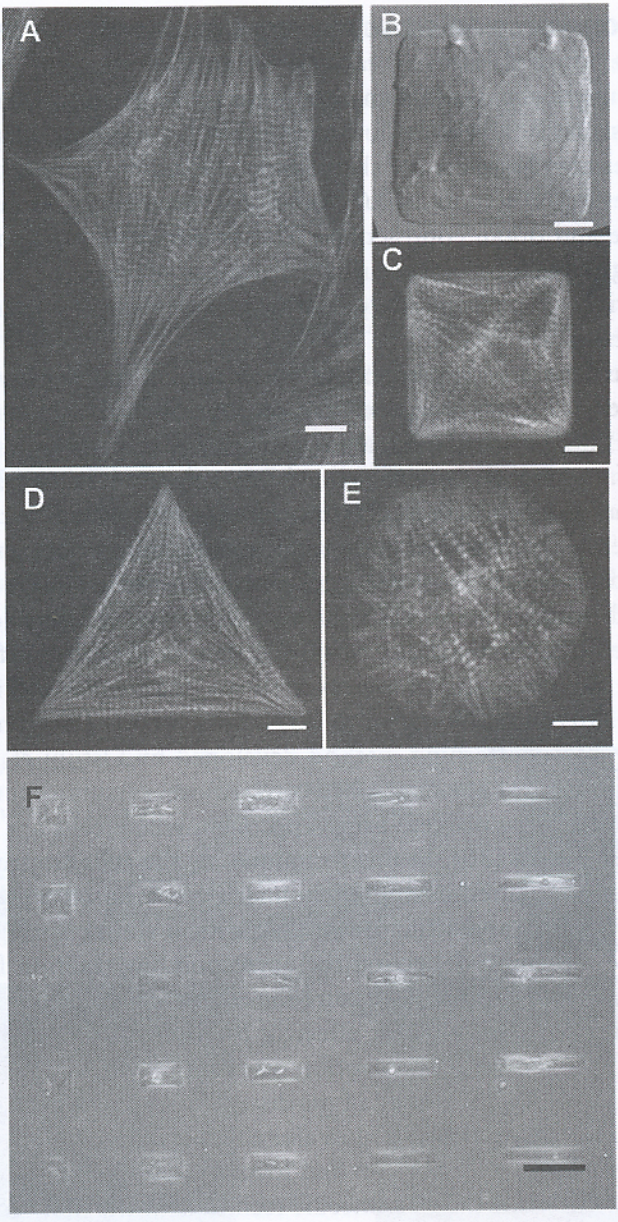

Figure 17.5 *Morphology of individual NNRVMs*: (a) NNRVMs plated at low density on a uniform monolayer of FN display a random shape and alignment of myofibrils. (b) Atomic force microscopy of living NNRVMs plated onto 50 × 50 μm square FN islands shows the myocyte maintains a relatively flat (~0.5 to 1 μm) structure along the edges, with a raised section (2.9 μm) corresponding to the location of the nucleus. (c) NNRVMs prepared identically to (b) take the shape of the island, and myofibrils align to the long axis and the edges of the pattern. Using this technique for micropatterning single myocytes, (d) triangular and (e) circular myocytes can be generated, each having different degrees of structural orientation based on imposed boundary conditions. Stains for (a–e) are phalloidin; sarcomeric α-actinin; DNA (DAPI). (f) Patterned myocytes (here, with varying aspect ratios) can be oriented closely to each other in culture, increasing throughput for experimental techniques. atomic force microscopy image in (b) were taken under physiological conditions with an MFP-3-D-IO (Asylum Research, USA). Scale bars for (a–e) are 10 μm; scale bar for (f) is 100 μm.

17.4 Traction Force Microscopy for Cardiac Myocytes

Cardiac myocytes are designed to contract in order to pump blood. As described previously, it has been hypothesized that the mechanical properties of individual myocytes may be related to their shape [29]. In particular, the tractional forces that myocytes exert on both the ECM and each other may play an important role in overall tissue and organ contractility. This relationship is important when considering the design of myocardial tissue constructs, as well as in understanding the regulation of a variety of pathophysiological processes such as hypertrophy, dilated cardiomyopathy, and heart failure.

Quantitative measurement of the tractional forces exerted by mammalian cells on the cell-substrate interface have been measured by the use of either a continuous surface [28] or a discrete array of vertical microneedles [30]. In the continuous-surface approach, the cell-culture substrate is embedded with fluorescent beads that can be tracked with fluorescence optical microscopy. The displacements of the beads are measured and then correlated to the deformations generated by cell contractions. From these data, a continuous force field is reconstructed by using standard numerical techniques for solving ill-posed problems. Balaban et al. [3] developed a similar approach by micropatterning the surface of the substrate to measure the contractile force exerted on one focal adhesion by a single cardiac myocyte. Recently, Wang et al. [31] combined the continuous-surface approach with the micropatterning method developed by Ostuni et al. [32] to measure the traction force of shape-controlled cells. Another method of measuring cellular tractional forces is the discrete-array approach, where cells are cultured on an array of elastomeric posts [30]. In this technique, as the cells contract, the displacement of the posts is measured using optical microscopy. Based on the predetermined material composition and structure of the posts, a simple spring equation is applied to relate the measured deflection the corresponding traction force. Zhao and Zhang [33] used this approach to measure the contractile force of a single cardiac myocyte. They validated the inotropic effect of β-adrenergic stimulators by showing that a greater subcellular force generation was exerted when myocytes were perfused with isoproterenol. The drawback of the discrete-array approach is that the density of the microneedles under the cell is low due to fabrication limitations. This limitation significantly affects cell adhesion and locomotion compared to a flat and continuous surface [34]. While the microneedle technique is the most computationally efficient from the perspective of the investigator, the spacing between the microneedles represents a formidable obstacle for use with cardiac myocytes as they lack the motile capabilities of other cells that can easily extend lamellipodia and reach across free space to adhere to the adjacent needle head. We have found traction force microscopy on a continuous substrate to be superior for examining the structure-function relationships in shape-controlled NNRVMs. Not only do these techniques represent an excellent methodology for understanding cell function, but combining them with methods to control and engineer the cell microenvironment allows the investigator to systematically study structure-function relationships in cell biology.

Here, we describe our method of quantitatively measuring the contractile force of micropatterned myocytes cultured on a continuous surface. In this approach, fluorescent beads are attached to the surface of a flat elastomer that is suitable for car-

diac myocyte cell culture and verified by atomic force microscopy [Figure 17.6(a, b)] as opposed to being embedded throughout the volume of the substrate. Using this substrate, the shape of cardiac myocytes can be controlled by μCP. High-speed fluorescence video microscopy imaging of substrate deformation (measured by bead movement) due to myocyte contraction is then analyzed by an algorithm modified from Schwarz et al. to estimate the contractile force field of the micropatterned myocytes [Figure 17.6(c, d)] [35].

17.4.1 Substrate Preparation for Traction Force Microscopy

In this technique, PDMS is prepared at a higher base:curing agent ratio in order to lower its stiffness. As before, the polymer is coated onto a glass coverslip for analysis with optical microscopy. A similarly prepared block of PDMS was measured with a Bohlin CVOR Rheometer (Malvern Instruments, Malvern, UK) and was found to have a bulk modulus of ~12 to 15 kPa; this modulus is assumed to be the same for the coated coverslips. Fluorescence latex beads that are 0.2 μm in diameter with an excitation-emission spectrum of λ_{ex} = 540 to 580 nm and λ_{em} = 608 to 683 nm (Molecular Probes, Eugene, OR) are diluted 1:5,000 into a (PBS) solution, pH 7.40. The PDMS-coated coverslips are ultraviolet-ozone treated (Model 342,

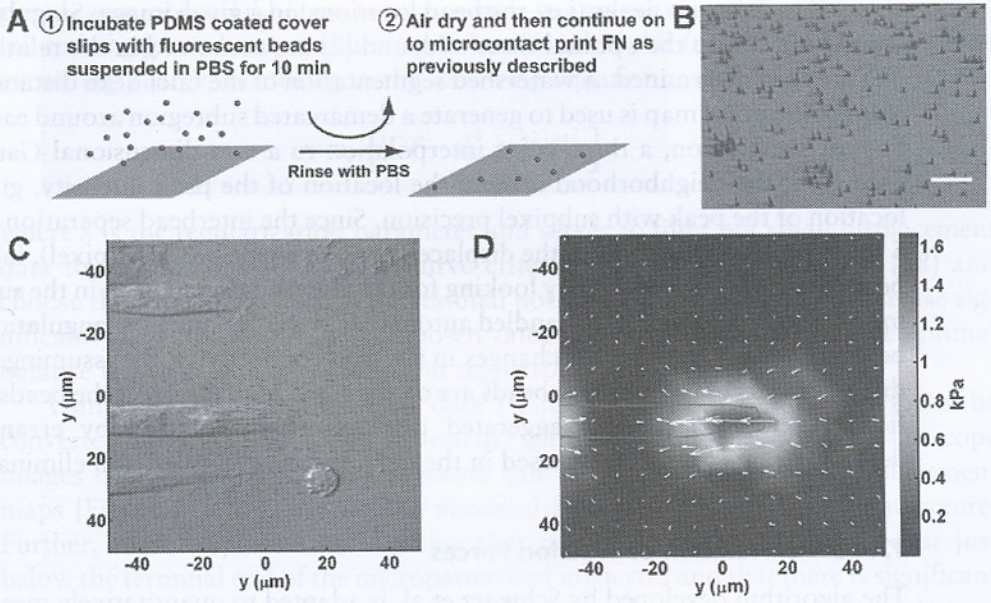

Figure 17.6 *Calculation of traction forces of micropatterned cardiac myocytes*: (a) Overview of the procedure for fabricating bead-coated PDMS substrates. (b) Atomic force micrograph of these substrates demonstrating a flat surface with 0.2 μm–diameter beads distributed across the surface. Scale bar = 5 ìm. (c) A DIC image of micropatterned myocytes superimposed with the displacements of the fluorescence beads. The myocytes were cultured on 10 μm micropatterned FN lines spaced 10 μm apart. The length and direction of the vectors represent the magnitude and the direction of bead displacements, respectively. The displacement vectors show that the substrate is pulled toward the longitudinal end of the myocyte but curled away at the middle of the cell. (d) The traction force map of the substrate. Relatively higher tractions are found to be concentrated at the long end of the myocyte.

Jelight Company, Irvine, CA) for two minutes and then incubated with the bead solution for ten minutes to allow bead attachment onto the surface of the PDMS. The bead solution is rinsed from the coverslip with PBS, air dried, and then micropatterned with FN using μCP as described in the section 17.3.3.

17.4.2 Identification and Tracking of Fluorescent Beads

Several image-processing procedures are involved in extracting the bead locations from the fluorescence image. A top-hat filter is applied to remove variations in the background intensity across an image. This also allows foreground objects (i.e., beads) that are smaller than a given size to be enhanced, while the intensity of background objects in the image is diminished. A thresholding approach [36] automatically determines an upper boundary (T_{UB}) grayscale value to define a bead in the image. The image is binarized with increasing threshold values to generate a curve composed of the average area of the thresholded regions as a function of threshold value. The lower boundary (T_{LB}) grayscale value is defined as that value where the average object area is maximum. The optimal threshold is finally selected as the maximum value in the range of $[T_{LB}, T_{UB}]$. Next, a generalized second-derivative test is used to detect relative intensity maxima within the image.

The grayscale image is converted into a phase map permitting the localization of singular points without regard to the local intensity [37]. These singular points correspond to intensity peaks (i.e., the bead locations) in a given image. Singular points that: (1) lie above the optimal threshold; and (2) are contained in the relative maxima are then determined. A watershed segmentation of the Euclidean distance transform of the point map is used to generate a demarcated subregion around each bead. For each subregion, a three-point interpolation to a two-dimensional Gaussian is used to fit the neighborhood around the location of the peak intensity, giving the location of the peak with subpixel precision. Since the interbead separation (usually 5 to 10 pixels) is bigger than the displacement of a single bead (~1 pixel), individual beads are tracked over time by looking for the closest detected bead in the successive image. Incorrect tracking is handled automatically via Delaunay triangulation of the bead points and looking for changes in the grid connectivity. By assuming that the displacements of neighboring beads are on the same spatial scale if the beads are sufficiently close together, exaggerated displacements produced by errant beads detected in one frame, but missed in the next, can be identified and eliminated.

17.4.3 Calculation of Traction Forces

The algorithm developed by Schwarz et al. is adapted to quantitatively measure the peak systolic forces of the patterned myocytes [35]. The substrate is considered to be an elastic half-space under tangential traction on the surface since the typical displacements of the beads are negligible (a few hundred nanometers) as compared to the substrate thickness (~50 μm). Because the substrates are assumed to be isotropic and incompressible, the Poisson's ratio (ν) is close to 0.5, and no out-of-plane deformations occur during tangential traction. Consequently, the whole elastic formulation becomes linear as well as two-dimensional and can therefore be described by a Fredholm integral equation of the first kind:

$$u_i(r) = \int dr' G_{ij}(r - r') F_j(r') \tag{17.1}$$

where $F(r')$ and $U(r')$ denote the stress and the displacement field, respectively; the summation is applied with $1 \leq i, J \leq 2$ since the problem is two-dimensional. In our case, is the Green function of the elastic isotropic half-space and can be derived from the Boussinesq solution:

$$G_{ij}(r) = \frac{3}{4\pi E r}\left(\delta_{ij} + \frac{x_i x_j}{r^2}\right) \tag{17.2}$$

where x_i represents the Cartesian coordinate of the displacement field referenced against a concentrated force exerted at the origin, $r \equiv \sqrt{x_i x_i}$, E is the Young modulus, and δ_{ij} is the Kronecker delta. The experimentally measured bead displacements are used to inversely solve the traction field from (17.1). A lattice composed of $8 \times 8\ \mu m^2$ squares is applied to the whole image to approximate the discretized localization of traction forces. Since the typical bead displacement is less than $1\ \mu m$ and the Young's modulus of the material is ~10 to 15 kPa, the approximated force points are separated at least by $4\ \mu m$, as suggested by Schwarz et al. [35]. The χ^2 statistics were employed to choose a solved force pattern such that its resultant displacement field is the best fit to the measured one. Since the inverse problem is ill posed, zero-order Tikhonov regularization is applied to stabilize the solution by minimizing χ^2 under the additional constraint that the forces should not become exceedingly large, according to the following equation:

$$\min_F \left\{ |GF - u|^2 + \lambda^2 |F|^2 \right\} \tag{17.3}$$

where λ is the regularization parameter and serves to filter out small displacement data to stabilize the solution. L-curve criterion is used to determine λ [38] and choose the value of λ at which the residual norm $R = |GF - u|^2$ starts to increase significantly as a function of λ. The chosen value of λ thus corresponds to the optimal balance between data agreement and regularization.

Using this, bead-displacement data from epifluorescence microscopy can be converted into tractional forces, as seen in Figure 17.6(c, d). DIC optical microscope images of a single contracting myocyte can be overlaid with bead-displacement maps [Figure 17.6(c)], relating the maximal displacement with cellular structure. Further, these displacements indicate that maximal tractional forces occur just below the terminal end of the micropatterened myocytes and that there is significant force transduction from the cell to the substratum. The advantage of this technique versus traditional methods that require the gluing of freshly harvested myocytes to the ends of suspended pipettes mounted in force transducers is that the previous method allowed only for the measurement of contraction along one axis, whereas traction force microscopy allows for examination of the functional consequences of myocyte shape, as well as a broad array of vector mathematical measurement of the traction field. Temporal data, such as the rate of contraction and relaxation, is easily handled by the image-analysis technique described, allowing examination of the behavior of subcompartments within the myocyte.

17.5 Conclusions and Future Perspectives

Understanding structure-function relationships is critical in cell biology in general, but it is of particular importance in the myocardium. Pathological examination of failing hearts reveals various changes in the cardiac tissue microenvironment that may provide clues in the search for new drug targets to curb the progression of cardiomyopathies and suppress arrhythmias. Alterations in the expression of ECM proteins, cell shape and alignment, and gap-junction distribution indicate that stress and strain patterns within the myocardium have contributed to both structural and electrical remodeling. To date, the geometric complexity of the heart and the unique dynamics of the cardiac tissue microenvironment have made it difficult to elucidate the mechanochemical and mechanoelectrical signaling pathways that underlie these events. Thus, new techniques developed from the materials sciences have made possible experiments involving the control of cellular structure to investigate the resulting effects on function and cell-ECM or cell-cell interactions [39]. In the heart, several pathologies are correlated to structural changes seen in myocytes [9, 40], suggesting that maladaptive remodeling on the single myocyte level produces regulatory or contractile dysfunction of the myocardial syncytium. Until the implementation of techniques to control cellular architecture and geometry by engineering the cell microenvironment, investigators did not possess the tools to control cellular structure to such a precise degree.

Microcontact printing represents a simple technique for controlling the cell microenvironment. For myocytes, control of myofibrillar architecture can be achieved at the single-cell and two-dimensional tissue level. Cardiac myocytes respond to ECM geometry by orienting their myofibrillar architecture based on micropatterned spatial cues, and this can be exploited to reconstitute structural phenotypes found in vivo in either healthy or failing hearts. Beyond the flexibility of experimental design imparted by these techniques, fabrication of two-dimensional and three-dimensional tissue constructs for regenerative purposes is also a focus of cell and tissue engineering [5].

The use of three-dimensional scaffolds [41, 42] and substrates [43–45] represents promising technologies for future understanding of cell dynamics in a three-dimensional environment. For example, it has been demonstrated not only that two-dimensional separation between cells is important for expression of connexin-43 and N-cadherin, but the vertical (i.e., depth) dimension of the substrate plays an important role in the proper expression and localization of these genes [44]. Further, expression of cell-attachment proteins and cytoskeletal structure seems to be altered when cells are cultured on a three-dimensional substratum rather than the traditional two-dimensional microenvironment [45]. These results suggest intriguing trends, and future work may result in a methodology to create three-dimensionally oriented tissues in vitro.

Within the past five years, innovations in the field of thermosensitive polymers has opened new prospects for tissue engineering by controlling the cell microenvironment. Shimizu et al. [46, 47] have developed a methodology for culturing cardiac myocytes on layers of poly(N-isopropylacrylimide) (PIPAAm), a thermosensitive, biocompatible polymer. Using this technique, cells are grown in vitro on a PIPAAm coated substrate and can be released by simply lowering the

temperatrure of the culture conditions rather than by traditional enzymatic degradation. Using this technique, pulsatile grafts of cardiac tissue are liberated from the culture substrate and can be used as needed. Combining these techniques with others that control the architecture and morphology of engineered tissue represents a powerful methodology for generating oriented, substrate, and scaffold-free muscle grafts.

Further advances in tissue engineering for myocardial tissues are manifest [48–54]. It is clear that the field has advanced greatly since the introduction of microfabrication and soft lithography techniques borrowed mainly from the materials sciences. Both two-dimensional and three-dimensional manipulation of the cell-culture microenvironment has greatly enhanced our understanding of structure-function relationships in the cell, particularly the cardiac myocyte. Not only do these techniques serve for making simplified models of individual cardiac myocytes, but extensions of these techniques can result in the fabrication of simple two-dimensional tissues and more complex pseudo-three-dimensional tissues free of the culture substrate/scaffold. Implementing a variety of these techniques will be a powerful means of understanding the function of the myocardium, as well as serve as a prelude to clinical and therapeutic applications of cardiac-tissue engineering.

Acknowledgments

The work presented here has been supported by the Harvard University Nanoscale Science and Engineering Center and the Harvard University Material Research Science and Engineering Centers of the National Science Foundation (NSF) under NSF award numbers PHY-0117795 and DMR-0213805, and by the Defense Advanced Research Projects Agency Biomolecular Motors Program, project number FA9550-05-1-0015 for engineered muscle activators cells and tissues.

ferences

[1] Chen, C. S., Mrksich, M., Huang, S., Whitesides, G. M., and Ingber, D. E., "Geometric control of cell life and death," *Science*, Vol. 276, 1997, pp. 1425–1428.

[2] Parker, K. K., Brock, A. L., Brangwynne, C., Mannix, R. J., Wang, N., Ostuni, E., Geisse, N. A., Adams, J. C., Whitesides, G. M., and Ingber, D. E., "Directional control of lamellipodia extension by constraining cell shape and orienting cell tractional forces," *Faseb J.*, Vol. 16, 2002, pp. 1195–1204.

[3] Balaban, N. Q., Schwarz, U. S., Riveline, D., Goichberg, P., Tzur, G., Sabanay, I., Mahalu, D., Safran, S., Bershadsky, A., Addadi, L., and Geiger, B., "Force and focal adhesion assembly: A close relationship studied using elastic micropatterned substrates," *Nat. Cell. Biol.*, Vol. 3, 2001, pp. 466–472.

[4] Bhatia, S. N., Balis, U. J., Yarmush, M. L., and Toner, M., "Effect of cell-cell interactions in preservation of cellular phenotype: Cocultivation of hepatocytes and nonparenchymal cells," *Faseb. J.*, Vol. 13, 1999, pp. 1883–1900.

[5] Khademhosseini, A., Langer, R., Borenstein, J., and Vacanti, J. P., "Microscale technologies for tissue engineering and biology," *Proc. Natl. Acad. Sci. USA*, Vol. 103, 2006, pp. 2480–2487.

[6] Spach, M. S., Heidlage, J. F., Dolber, P. C., and Barr, R. C., "Electrophysiological effects of remodeling cardiac gap junctions and cell size: Experimental and model studies of normal cardiac growth," *Circ. Res.*, Vol. 86, 2000, pp. 302–311.

[7] Kleber, A. G., and Rudy, Y., "Basic mechanisms of cardiac impulse propagation and associated arrhythmias," *Physiol. Rev.*, Vol. 84, 2004, pp. 431–488.

[8] Spach, M. S., Miller, W. T., III, Geselowitz, D. B., Barr, R. C., Kootsey, J. M., and Johnson, E. A., "The discontinuous nature of propagation in normal canine cardiac muscle: Evidence for recurrent discontinuities of intracellular resistance that affect the membrane currents," *Circ. Res.*, Vol. 48, 1981, pp. 39–54.

[9] Gerdes, A. M., and Capasso, J. M., "Structural remodeling and mechanical dysfunction of cardiac myocytes in heart failure," *J. Mol. Cell. Cardiol.*, Vol. 27, 1995, pp. 849–856.

[10] Lammerding, J., Kamm, R. D., and Lee, R. T., "Mechanotransduction in cardiac myocytes," *Annals NY Acad. Sci.*, Vol. 1015, 2004, pp. 53–70.

[11] Lieberman, M., Roggeveen, A. E., Purdy, J. E., and Johnson, E. A., "Synthetic strands of cardiac muscle: Growth and physiological implication," *Science*, Vol. 175, 1972, pp. 909–911.

[12] Lieberman, M., Sawanobori, T., Kootsey, J. M., and Johnson, E. A., "A synthetic strand of cardiac muscle: Its passive electrical properties," *J. Gen. Physiol.*, Vol. 65, 1975, pp. 527–550.

[13] Bursac, N., Parker, K. K., Iravanian, S., and Tung, L., "Cardiomyocyte cultures with controlled macroscopic anisotropy: A model for functional electrophysiological studies of cardiac muscle," *Circ. Res.*, Vol. 91, 2002, pp. e45–e54.

[14] Xia, Y., and Whitesides, G. M., "Soft lithography," *Angewandte Chemie—Inter. Ed.*, Vol. 37, 1998, pp. 550–575.

[15] Whitesides, G. M., Ostuni, E., Takayama, S., Jiang, X., and Ingber, D. E., "Soft lithography in biology and biochemistry," *Ann. Rev. Biomed. Eng.*, Vol. 3, 2001, pp. 335–373.

[16] Rohr, S., Scholly, D. M., and Kleber, A. G., "Patterned growth of neonatal rat heart cells in culture: Morphological and electrophysiological characterization," *Circ. Res.*, Vol. 68, 1991, pp. 114–130.

[17] Rohr, S., Kleber, A. G., and Kucera, J. P., "Optical recording of impulse propagation in designer cultures: Cardiac tissue architectures inducing ultra-slow conduction," *Trends Cardiovasc. Med.*, Vol. 9, 1999, pp. 173–179.

[18] Gillis, A. M., Fast, V. G., Rohr, S., and Kleber, A. G., "Mechanism of ventricular defibrillation: The role of tissue geometry in the changes in transmembrane potential in patterned myocyte cultures," *Circulation*, Vol. 101, 2000, pp. 2438–2445.

[19] Kaplan, S. R., Gard, J. J., Protonotarios, N., Tsatsopoulou, A., Spiliopoulou, C., Anastasakis, A., Squarcioni, C. P., McKenna, W. J., Thiene, G., Basso, C., Brousse, N., Fontaine, G., and Saffitz, J. E., "Remodeling of myocyte gap junctions in arrhythmogenic right ventricular cardiomyopathy due to a deletion in plakoglobin (Naxos disease)." *Heart Rhythm*, Vol. 1, 2004, pp. 3–11.

[20] Kaplan, S. R., Gard, J. J., Carvajal-Huerta, L., Ruiz-Cabezas, J. C., Thiene, G., and Saffitz, J. E., "Structural and molecular pathology of the heart in Carvajal syndrome," *Cardiovasc. Pathol.*, Vol. 13, 2004, pp. 26–32.

[21] Kanno, S., and Saffitz, J. E., "The role of myocardial gap junctions in electrical conduction and arrhythmogenesis," *Cardiovasc. Pathol.*, Vol. 10, 2001, pp. 169–177.

[22] Sathaye, A., Bursac, N., Sheehy, S., and Tung, L., "Electrical pacing counteracts intrinsic shortening of action potential duration of neonatal rat ventricular cells in culture," *J. Mol. Cell. Cardiol.*, Vol. 41, 2006, pp. 633–641.

[23] Lipp, P., and Niggli, E., "Modulation of Ca
release in cultured neonatal rat cardiac myocytes: Insight from subcellular release patterns revealed by confocal microscopy," *Circ. Res.*, Vol. 74, 1994, pp. 979–990.

[24] Kennedy, R. A., Kemp, T. J., Sugden, P. H., and Clerk, A., "Using U0126 to dissect the role of the extracellular signal-regulated kinase 1/2 (ERK1/2) cascade in the regulation of gene expression by endothelin-1 in cardiac myocytes," *J. Mol. Cell. Cardiol.*, Vol. 41, 2006, pp. 236–247.

[25] Arutunyan, A., Swift, L. M., and Sarvazyan, N., "Initiation and propagation of ectopic waves: Insights from an in vitro model of ischemia-reperfusion injury," *Am. J. Physiol.: Heart Circ. Physiol.*, Vol. 283, 2002, pp. H741–H749.

[26] Simpson, P., "Norepinephrine-stimulated hypertrophy of cultured rat myocardial cells is an alpha 1 adrenergic response," *J. Clin. Invest.*, Vol. 72, 1983, pp. 732–738.

[27] Tan, J. L., Liu, W., Nelson, C. M., Raghavan, S., and Chen, C. S., "Simple approach to micropattern cells on common culture substrates by tuning substrate wettability," *Tissue Eng.*, Vol. 10, 2004, pp. 865–872.

[28] Dembo, M., and Wang, Y. L., "Stresses at the cell-to-substrate interface during locomotion of fibroblasts," *Biophys. J.*, Vol. 76, 1999, pp. 2307–2316.

[29] Russell, B., Motlagh, D., and Ashley, W. W., "Form follows function: How muscle shape is regulated by work," *J. Appl. Physiol.*, Vol. 88, 2000, pp. 1127–1132.

[30] Tan, J. L., Tien, J., Pirone, D. M., Gray, D. S., Bhadriraju, K., and Chen, C. S., "Cells lying on a bed of microneedles: An approach to isolate mechanical force," *Proc. Natl. Acad. Sci. USA*, Vol. 100, 2003, pp. 1484–1489.

[31] Wang, N., Ostuni, E., Whitesides, G. M., and Ingber, D. E., "Micropatterning tractional forces in living cells," *Cell Motil. Cytoskeleton*, Vol. 52, 2002, pp. 97–106.

[32] Ostuni, E., Kane, R., Chen, C. S., Ingber, D. E., and Whitesides, G. M., "Patterning mammalian cells using elastomeric membranes," *Langmuir*, Vol. 16, 2000, pp. 7811–7819.

[33] Zhao, Y., and Zhang, X., "Cellular mechanics study in cardiac myocytes using PDMS pillars array," *Sens. Actuators A: Physical*, Vol. 125, 2006, pp. 398–404.

[34] du Roure, O., Saez, A., Buguin, A., Austin, R. H., Chavrier, P., Silberzan, P., and Ladoux, B., "Force mapping in epithelial cell migration," *Proc. Natl. Acad. Sci. USA*, Vol. 102, 2005, pp. 2390–2395.

[35] Schwarz, U. S., Balaban, N. Q., Riveline, D., Bershadsky, A., Geiger, B., and Safran, S. A., "Calculation of forces at focal adhesions from elastic substrate data: The effect of localized force and the need for regularization," *Biophys. J.*, Vol. 83, 2002, pp. 1380–1394.

[36] Otsu, N., "A thresholding selection method from gray-level histogram," *IEEE Trans. Syst. Man Cybernet.*, Vol. 9, 1979, pp. 62–66.

[37] Bray, M. A., Lin, S. F., Aliev, R. R., Roth, B. J., and Wikswo, J. P., Jr., "Experimental and theoretical analysis of phase singularity dynamics in cardiac tissue," *J. Cardiovasc. Electrophysiol.*, Vol. 12, 2001, pp. 716–722.

[38] Hansen, P. C., "Rank-deficient and discrete ill-posed problems: Numerical aspects of linear inversion," *Society for Industrial and Applied Mathematics*, Philadelphia, PA, 1997.

[39] Raghavan, S., and Chen, C. S., "Micropatterned environments in cell biology," *Adv. Mater.*, Vol. 16, 2004, pp. 1303–1313.

[40] Gerdes, A. M., "Cardiac myocyte remodeling in hypertrophy and progression to failure," *J. Card. Fail.*, Vol. 8, 2002, pp. S264–S268.

[41] Christman, K. L., and Lee, R. J., "Biomaterials for the treatment of myocardial infarction," *J. Am. Coll. Cardiol.*, Vol. 48, 2006, pp. 907–913.

[42] Park, H., Radisic, M., Lim, J. O., Chang, B. H., and Vunjak-Novakovic, G., "A novel composite scaffold for cardiac tissue engineering," *In Vitro Cell. Dev. Biol.: Anim.*, Vol. 41, 2005, pp. 188–196.

[43] Deutsch, J., Motlagh, D., Russell, B., and Desai, T. A., "Fabrication of microtextured membranes for cardiac myocyte attachment and orientation," *J. Biomed. Mater. Res.*, Vol. 53, 2000, pp. 267–275.

[44] Motlagh, D., Hartman, T. J., Desai, T. A., and Russell, B., "Microfabricated grooves recapitulate neonatal myocyte connexin43 and N-cadherin expression and localization," *J. Biomed. Mater. Res. A*, Vol. 67, 2003, pp. 148–157.

[45] Motlagh, D., Senyo, S. E., Desai, T. A., and Russell, B., "Microtextured substrata alter gene expression, protein localization and the shape of cardiac myocytes," *Biomaterials*, Vol. 24, 2003, pp. 2463–2476.

[46] Shimizu, T., Yamato, M., Isoi, Y., Akutsu, T., Setomaru, T., Abe, K., Kikuchi, A., Umezu, M., and Okano, T., "Fabrication of pulsatile cardiac tissue grafts using a novel 3-dimensional cell sheet manipulation technique and temperature-responsive cell culture surfaces," *Circ. Res.*, Vol. 90, 2002, p. e40.

[47] Shimizu, T., Sekine, H., Isoi, Y., Yamato, M., Kikuchi, A., and Okano, T., "Long-term survival and growth of pulsatile myocardial tissue grafts engineered by the layering of cardiomyocyte sheets," *Tissue Eng.*, Vol. 12, 2006, pp. 499–507.

[48] Radisic, M., Park, H., Shing, H., Consi, T., Schoen, F. J., Langer, R., Freed, L. E., and Vunjak-Novakovic, G., "Functional assembly of engineered myocardium by electrical stimulation of cardiac myocytes cultured on scaffolds," *Proc. Natl. Acad. Sci. USA*, Vol. 101, 2004, pp. 18129–18134.

[49] Zimmermann, W. H., Schneiderbanger, K., Schubert, P., Didie, M., Munzel, F., Heubach, J. F., Kostin, S., Neuhuber, W. L., and Eschenhagen, T., "Tissue engineering of a differentiated cardiac muscle construct," *Circ. Res.*, Vol. 90, 2002, pp. 223–230.

[50] Leor, J., Aboulafia-Etzion, S., Dar, A., Shapiro, L., Barbash, I. M., Battler, A., Granot, Y., and Cohen, S., "Bioengineered cardiac grafts: A new approach to repair the infarcted myocardium?" *Circulation*, Vol. 102, 2000, pp. III56–III61.

[51] Carrier, R. L., Papadaki, M., Rupnick, M., Schoen, F. J., Bursac, N., Langer, R., Freed, L. E., and Vunjak-Novakovic, G., "Cardiac tissue engineering: Cell seeding, cultivation parameters, and tissue construct characterization," *Biotechnol. Bioeng.*, Vol. 64, 1999, pp. 580–589.

[52] Papadaki, M., Bursac, N., Langer, R., Merok, J., Vunjak-Novakovic, G., and Freed, L. E., "Tissue engineering of functional cardiac muscle: Molecular, structural, and electrophysiological studies," *Am. J. Physiol.: Heart Circ. Physiol.*, Vol. 280, 2001, pp. H168–H178.

[53] Eschenhagen, T., Fink, C., Remmers, U., Scholz, H., Wattchow, J., Weil, J., Zimmermann, W., Dohmen, H. H., Schafer, H., Bishopric, N., Wakatsuki, T., and Elson, E. L., "Three-dimensional reconstitution of embryonic cardiomyocytes in a collagen matrix: A new heart muscle model system," *Faseb. J.*, Vol. 11, 1997, pp. 683–694.

[54] Khademhosseini, A., Eng, G., Yeh, J., Kucharczyk, P. A., Langer, R., Vunjak-Novakovic, G., and Radisic, M., "Microfluidic patterning for fabrication of contractile cardiac organoids," *Biomed. Microdevices*, Vol. 9, 2007, pp. 149–157.